

Single-ion versus exchange anisotropy in calculating anisotropic susceptibilities of thin ferromagnetic Heisenberg films within many-body Green's function theory

P. Fröbrich⁺, and P.J. Kuntz

Hahn-Meitner-Institut Berlin, Glienicker Straße 100, D-14109 Berlin, Germany,

⁺also: Institut für Theoretische Physik, Freie Universität Berlin

Arnimallee 14, D-14195 Berlin, Germany

Abstract. We compare transverse and parallel static susceptibilities of in-plane uniaxial anisotropic ferromagnetic Heisenberg films calculated in the framework of many-body Green's function theory using single-ion anisotropies with the previously investigated case of exchange anisotropies. On the basis of the calculated observables (easy and hard axes magnetizations and susceptibilities) no significant differences are found, i.e. it is *not* possible to propose an experiment that might decide which kind of anisotropy is acting in an actual ferromagnetic film.

PACS. 75.10.Jm Quantized spin models - 75.30.Ds Spin waves - 75.70.Ak Magnetic properties of monolayers and thin films

1. Introduction

Jensen et al. [1] have measured parallel and tranverse susceptibilities of a bi-layer Co film with an *in-plane* uniaxial anisotropy, and analysed their results with a many-body Green's function theory assuming a spin value of $S = 1/2$. We have generalized their work to multilayers and arbitrary spin in Ref. [2]. In both papers an exchange anisotropy was used, because it is easier to treat than the single-ion anisotropy. In connection with the reorientation of the magnetization of a ferromagnetic film (with an *out-of-plane* anisotropy) as function of the temperature and film thickness we have already discussed similarities and differences between single-ion and exchange anisotropies [3]. In the latter paper the magnetic dipole-dipole interaction was also included.

In the present paper we calculate within the Green's function formalism anisotropic in-plane susceptibilities using the single-ion anisotropy, and compare with the results of Ref. [2], where the exchange anisotropy was used. Although we have shown in Ref. [4] how the single-ion anisotropy can be treated exactly (for any strength of the anisotropy) by introducing higher-order Green's functions, the application to multilayers and $S > 1$ is very cumbersome. This is not the case when using, as we did in Refs. [3] and [5] and we do in the present paper, an approximate decoupling on the level of the lowest-order Green's functions proposed by Anderson and Callen [6], which however is only a good approximation for small anisotropies, as we showed in Ref. [7] by comparing with 'exact' Quantum Monte Carlo calculations. In keeping with Refs. [1] and [2] we do not include the dipole-dipole interaction, because it is nearly isotropic for an in-plane situation.

The paper is organized as follows. In Section 2 we explain the model and establish the Green's function formalism. Section 3 displays the numerical results. In Section 4 we summarize the results and present our conclusions.

2. The model and the Green's function formalism

Although the general formalism is rather similar to our previous work we repeat it here to make the paper self-contained.

The Hamiltonian we use in this paper consists of an isotropic Heisenberg exchange interaction with strength J_{kl} between nearest neighbour lattice sites, a second-order *in-plane* single-ion lattice anisotropy with strength $K_{2,k}$, and an external magnetic field $\mathbf{B} = (B^x, B^y, B^z)$:

$$\mathcal{H} = - \frac{1}{2} \sum_{\langle kl \rangle} J_{kl} (S_k^- S_l^+ + S_k^z S_l^z) - \sum_k K_{2,k} (S_k^z)^2$$

$$- \sum_k \left(\frac{1}{2} B^- S_k^+ + \frac{1}{2} B^+ S_k^- + B^z S_k^z \right). \quad (1)$$

Here the notation $S_k^\pm = S_k^x \pm i S_k^y$ and $B^\pm = B^x \pm i B^y$ is introduced, where k and l are lattice site indices and $\langle kl \rangle$ indicates summation over nearest neighbours only. The in-plane lattice directions are the x and z-axes. The field B^y will be put to zero lateron.

In order to treat the problem for general spin S , we need the following Green's functions

$$G_{ij,\eta}^{\alpha,mn}(\omega) = \langle \langle S_i^\alpha; (S_j^z)^m (S_j^-)^n \rangle \rangle_{\omega,\eta}, \quad (2)$$

where $\alpha = (+, -, z)$ takes care of all directions in space, $\eta = \pm 1$ refers to the anticommutator or commutator Green's functions, respectively, and $n \geq 1, m \geq 0$ are positive integers, necessary for dealing with higher spin values S .

The exact equations of motion are

$$\omega G_{ij,\eta}^{\alpha,mn}(\omega) = A_{ij,\eta}^{\alpha,mn} + \langle \langle [S_i^\alpha, \mathcal{H}]_-; (S_j^z)^m (S_j^-)^n \rangle \rangle_{\omega,\eta} \quad (3)$$

with the inhomogeneities

$$A_{ij,\eta}^{\alpha,mn} = \langle [S_i^\alpha, (S_j^z)^m (S_j^-)^n]_\eta \rangle, \quad (4)$$

where $\langle \dots \rangle = Tr(\dots e^{-\beta \mathcal{H}}) / Tr(e^{-\beta \mathcal{H}})$. The equations are given explicitly by

$$\begin{aligned} \omega G_{ij,\eta}^{\pm,mn} &= A_{ij,\eta}^{\pm,mn} \\ &\mp \sum_k J_{ik} \left(\langle \langle S_i^z S_k^\pm; (S_j^z)^m (S_j^-)^n \rangle \rangle - \langle \langle S_k^z S_i^\pm; (S_j^z)^m (S_j^-)^n \rangle \rangle \right) \\ &\pm K_{2,i} \langle \langle (S_i^\pm S_i^z + S_i^z S_i^\pm); (S_j^z)^m (S_j^-)^n \rangle \rangle \\ &\mp B^\pm G_{ij,\eta}^{z,mn} \pm B^z G_{ij,\eta}^{\pm,mn} \\ \omega G_{ij,\eta}^{z,mn} &= A_{ij(\eta)}^{z,mn} \\ &+ \frac{1}{2} \sum_k J_{ik} \langle \langle (S_i^- S_k^+ - S_k^- S_i^+); (S_j^z)^m (S_j^-)^n \rangle \rangle \\ &- \frac{1}{2} B^- G_{ij,\eta}^{+,mn} + \frac{1}{2} B^+ G_{ij,\eta}^{-,mn}. \end{aligned} \quad (5)$$

After solving these equations the components of the magnetization can be determined from the Green's functions via the spectral theorem. A solution is possible by establishing a closed system of equations by decoupling the higher-order Green's functions on the right-hand sides. Contrary to Ref. [4], where we proceed to higher-order Green's functions, we stay here at the level of the lowest-order equations. For the exchange-interaction terms, we use a generalized Tyablikov- (or RPA-) decoupling

$$\langle \langle S_i^\alpha S_k^\beta; (S_j^z)^m (S_j^-)^n \rangle \rangle_\eta \simeq \langle S_i^\alpha \rangle G_{kj,\eta}^{\beta,mn} + \langle S_k^\beta \rangle G_{ij,\eta}^{\alpha,mn}. \quad (6)$$

The terms from the single-ion anisotropy have to be decoupled differently, because an RPA decoupling leads to unphysical results; e.g. for spin $S = 1/2$, the terms due to the single-ion anisotropy do not vanish in RPA, as they should do, because in this case $\sum_i K_{2,i} \langle (S_i^z)^2 \rangle$ is a constant and should not influence the equations of motion. In the appendix of Ref. [8] we investigated different decoupling schemes proposed in the literature, e.g. those of Lines [9] or that of Anderson and Callen [6], which should be reasonable for single-ion anisotropies small compared to the exchange interaction. We found the Anderson-Callen decoupling to be most adequate. It consists in implementing the suggestion of Callen [10] to improve the RPA by treating the diagonal terms arising from the single-ion anisotropy as well. This leads to

$$\begin{aligned} & \langle \langle (S_i^\pm S_i^z + S_i^z S_i^\pm); (S_j^z)^m (S_j^-)^n \rangle \rangle_\eta \\ & \simeq 2 \langle S_i^z \rangle \left(1 - \frac{1}{2S^2} [S(S+1) - \langle S_i^z S_i^z \rangle] \right) G_{ij,\eta}^{\pm,mn}. \end{aligned} \quad (7)$$

This term vanishes for $S = 1/2$ as it should.

After a Fourier transform to momentum space, one obtains, for a ferromagnetic film with N layers, $3N$ equations of motion for a $3N$ -dimensional Green's function vector \mathbf{G}^{mn} :

$$(\omega \mathbf{1} - \mathbf{\Gamma}) \mathbf{G}^{mn} = \mathbf{A}^{mn}, \quad (8)$$

where $\mathbf{1}$ is the $3N \times 3N$ unit matrix. The Green's function vectors and inhomogeneity vectors each consist of N three-dimensional subvectors which are characterized by the layer indices i and j

$$\mathbf{G}_{ij}^{mn}(\mathbf{k}, \omega) = \begin{pmatrix} G_{ij}^{+,mn}(\mathbf{k}, \omega) \\ G_{ij}^{-,mn}(\mathbf{k}, \omega) \\ G_{ij}^{z,mn}(\mathbf{k}, \omega) \end{pmatrix}, \quad \mathbf{A}_{ij}^{mn} = \begin{pmatrix} A_{ij}^{+,mn} \\ A_{ij}^{-,mn} \\ A_{ij}^{z,mn} \end{pmatrix}. \quad (9)$$

The equations of motion are then expressed in terms of these layer vectors, and 3×3 submatrices $\mathbf{\Gamma}_{ij}$ of the $3N \times 3N$ matrix $\mathbf{\Gamma}$

$$\left[\omega \mathbf{1} - \begin{pmatrix} \mathbf{\Gamma}_{11} & \mathbf{\Gamma}_{12} & \dots & \mathbf{\Gamma}_{1N} \\ \mathbf{\Gamma}_{21} & \mathbf{\Gamma}_{22} & \dots & \mathbf{\Gamma}_{2N} \\ \dots & \dots & \dots & \dots \\ \mathbf{\Gamma}_{N1} & \mathbf{\Gamma}_{N2} & \dots & \mathbf{\Gamma}_{NN} \end{pmatrix} \right] \begin{bmatrix} \mathbf{G}_{1j} \\ \mathbf{G}_{2j} \\ \dots \\ \mathbf{G}_{Nj} \end{bmatrix} = \begin{bmatrix} \mathbf{A}_{1j} \delta_{1j} \\ \mathbf{A}_{2j} \delta_{2j} \\ \dots \\ \mathbf{A}_{Nj} \delta_{Nj} \end{bmatrix}, \quad j = 1, \dots, N. \quad (10)$$

After applying the decoupling procedures (6) and (7), the $\mathbf{\Gamma}$ matrix reduces to a band matrix with zeros in the $\mathbf{\Gamma}_{ij}$ sub-matrices, when $j > i + 1$ and $j < i - 1$. The

diagonal sub-matrices Γ_{ii} are of size 3×3 and have the form

$$\Gamma_{ii} = \begin{pmatrix} H_i^z & 0 & -H_i^+ \\ 0 & -H_i^z & H_i^- \\ -\frac{1}{2}H_i^- & \frac{1}{2}H_i^+ & 0 \end{pmatrix}. \quad (11)$$

where

$$\begin{aligned} H_i^z &= Z_i + \langle S_i^z \rangle J_{ii}(q - \gamma_{\mathbf{k}}), \\ Z_i &= B_i^z + J_{i,i+1} \langle S_{i+1}^z \rangle + J_{i,i-1} \langle S_{i-1}^z \rangle \\ &\quad + K_{2,i} 2 \langle S_i^z \rangle \left(1 - \frac{1}{2S^2} [S(S+1) - \langle S_i^z S_i^z \rangle] \right), \\ H_i^\pm &= B_i^\pm + \langle S_i^\pm \rangle J_{ii}(q - \gamma_{\mathbf{k}}) + J_{i,i+1} \langle S_{i+1}^\pm \rangle + J_{i,i-1} \langle S_{i-1}^\pm \rangle. \end{aligned} \quad (12)$$

For a square lattice, to which we restrict ourselves in the present paper, and a lattice constant taken to be unity, $\gamma_{\mathbf{k}} = 2(\cos k_x + \cos k_y)$, and $q = 4$ is the number of intra-layer nearest neighbours.

The 3×3 off-diagonal sub-matrices Γ_{ij} for $j = i \pm 1$ are of the form

$$\Gamma_{ij} = \begin{pmatrix} -J_{ij} \langle S_i^z \rangle & 0 & J_{ij} \langle S_i^+ \rangle \\ 0 & J_{ij} \langle S_i^z \rangle & -J_{ij} \langle S_i^- \rangle \\ \frac{1}{2} J_{ij} \langle S_i^- \rangle & -\frac{1}{2} J_{ij} \langle S_i^+ \rangle & 0 \end{pmatrix}. \quad (13)$$

When treating the monolayer, one can use the spectral theorem for calculating the components of the magnetization. This was done in Ref. [8] for the case of spin $S = 1$ and an out-of-plane single-ion anisotropy by using the commutator Green's functions. In order to obtain sufficient equations it was necessary, to add equations coming from the condition that the commutator Green's functions have to be regular at $\omega = 0$, which we call the regularity conditions.

The treatment of multilayers is only practicable when using the eigenvector method developed in Ref. [5]. The essential features are as follows. One starts with a transformation, which diagonalizes the Γ -matrix of equation (8)

$$\mathbf{L} \mathbf{\Gamma} \mathbf{R} = \mathbf{\Omega}, \quad (14)$$

where $\mathbf{\Omega}$ is a diagonal matrix with eigenvalues ω_τ ($\tau = 1, \dots, 3N$). For the problem above it turns out that there is one eigenvalue equal to zero for each layer, which has to be handled appropriately. The transformation matrix \mathbf{R} and its inverse $\mathbf{R}^{-1} = \mathbf{L}$ are obtained from the right eigenvectors of $\mathbf{\Gamma}$ as columns and from the left eigenvectors as rows, respectively. These matrices are normalized to unity: $\mathbf{R} \mathbf{L} = \mathbf{L} \mathbf{R} = \mathbf{1}$.

Multiplying the equation of motion (8) from the left by \mathbf{L} and inserting $\mathbf{1}=\mathbf{RL}$ one finds

$$(\omega\mathbf{1} - \Omega)\mathbf{L}\mathbf{G}_\eta^{mn} = \mathbf{L}\mathbf{A}_\eta^{mn}. \quad (15)$$

Defining $\mathcal{G}_\eta^{mn} = \mathbf{L}\mathbf{G}_\eta^{mn}$ and $\mathcal{A}_\eta^{mn} = \mathbf{L}\mathbf{A}_\eta^{mn}$ one obtains

$$(\omega\mathbf{1} - \Omega)\mathcal{G}_\eta^{mn} = \mathcal{A}_\eta^{mn}. \quad (16)$$

\mathcal{G}_η^{mn} is a vector of new Green's functions, each component τ of which has but a single pole

$$\mathcal{G}_\eta^{mn,\tau} = \frac{\mathcal{A}_\eta^{mn,\tau}}{\omega - \omega_\tau}. \quad (17)$$

This is the important point because it allows application of the spectral theorem, e.g. [11], to each component separately. We obtain for the component τ of correlation vector $\mathcal{C}^{mn} = \mathbf{L}\mathbf{C}^{mn}$ (where $\mathbf{C}^{mn} = \langle (S^z)^m (S^-)^n S^\alpha \rangle$ with $(\alpha = +, -, z)$)

$$\mathcal{C}^{mn,\tau} = \frac{\mathcal{A}_\eta^{mn,\tau}}{e^{\beta\omega_\tau} + \eta} + \frac{1}{2}(1 - \eta)\frac{1}{2} \lim_{\omega \rightarrow 0} \omega \frac{\mathcal{A}_{\eta=+1}^{mn,\tau}}{\omega - \omega_\tau}. \quad (18)$$

We emphasize that when $(\eta = -1)$, the second term of this equation, which is due to the anticommutator Green's function, has to be taken into account. This term occurs for $\omega_\tau = 0$ and can be simplified by using the relation between anticommutator and commutator

$$\mathcal{A}_{\eta=+1}^{mn,0} = \mathcal{A}_{\eta=-1}^{mn,0} + 2\mathcal{C}^{mn,0} = \mathbf{L}_0(A_{\eta=-1}^{mn} + 2\mathbf{C}^{mn}), \quad (19)$$

where the index $\tau = 0$ refers to the eigenvector with $\omega_\tau = 0$.

The term $\mathbf{L}_0 A_{\eta=-1}^{mn} = 0$ vanishes due to the fact that the commutator Green's function has to be regular at the origin

$$\lim_{\omega \rightarrow 0} \omega G_{\eta=-1}^{\alpha,mn} = 0, \quad (20)$$

which leads to the regularity conditions:

$$H^x A_{\eta=-1}^{+,mn} + H^x A_{\eta=-1}^{-,mn} + 2H^z A_{\eta=-1}^{z,mn} = 0. \quad (21)$$

For details, see Ref. [5].

This is equivalent to

$$\mathbf{L}_0 A_{\eta=-1}^{mn} = 0, \quad (22)$$

because the left eigenvector of the Γ -matrix with eigenvector zero has the structure

$$\mathbf{L}_0 \propto (H^x, H^x, 2H^z), \quad (23)$$

what can be seen analytically. For more details concerning the use of the regularity conditions, see Refs. [2, 5].

We mention an alternative method, published in Ref. [12], of treating zero eigenvalues occurring in the equation of motion matrix, which is based on a singular value decomposition of this matrix, and where there is no need for the use of the anticommutator Green's function.

The equations for the correlations are obtained by multiplying equation (18) from the left with \mathbf{R} and using equation (22); i.e.

$$\mathbf{C} = \mathbf{R}\mathcal{E}\mathbf{L}\mathbf{A} + \mathbf{R}_0\mathbf{L}_0\mathbf{C}, \quad (24)$$

where \mathcal{E} is a diagonal matrix with matrix elements $\mathcal{E}_{ij} = \delta_{ij}(e^{\beta\omega_i} - 1)^{-1}$ for eigenvalues $\omega_i \neq 0$, and 0 for eigenvalues $\omega_i = 0$.

This set of equations has to be solved self-consistently together with the regularity conditions (21). This determines the magnetizations and the moments of the magnetizations $\langle (S^z)^n \rangle$ with $n = 2S + 1$ for the highest moment, S being the spin quantum number. For details see Appendix A of Ref. [3], where an analogous set of similar equations is given more explicitly for the case of the out-of-plane situation.

The susceptibilities with respect to the easy (χ_{zz}) and hard (χ_{xx}) axes are calculated as differential quotients

$$\begin{aligned} \chi_{zz} &= \left(\langle S^z(B^z) \rangle - \langle S^z(0) \rangle \right) / B^z \\ \chi_{xx} &= \left(\langle S^x(B^x) \rangle - \langle S^x(0) \rangle \right) / B^x, \end{aligned} \quad (25)$$

where the use of $B^{z(x)} = 0.01/S$ turns out to be small enough, see also Ref. [2].

3. Numerical results

In this section we show numerical results obtained with the single-ion anisotropy in comparison with that from the exchange anisotropy, for which the relevant equations were derived in Ref. [2]. As the single-ion anisotropy is not active for $S = 1/2$ we will show results for $S \geq 1$. In an attempt to obtain universal (independent of the spin quantum number S) curves, we have scaled the parameters ($J, D, B^{x(z)}$) entering the Hamiltonian of Ref. [2] as $\tilde{J}/S(S+1) = J$, $\tilde{D}/S(S+1) = D$ (D being the strength of the exchange anisotropy), $\tilde{B}^{x(z)}/S = B^{x(z)}$. In the present paper we use an additional scaling for the strength of the single-ion anisotropy $\tilde{K}_2/(S-1/2) = K_2$. This has been proven to be the proper scaling in Ref.[5], because it leads to the correct limit $\lim_{T \rightarrow 0} (K_2(T)/K_2(0)) = 1$, when calculating the temperature- dependent anisotropy by minimizing the free energy with respect to the equilibrium orientation angle of the magnetization.

3.1 The monolayer with arbitrary spin

In order to compare results obtained with the single-ion anisotropy and with the exchange anisotropy we fit the strength of the single-ion anisotropy to $K_2 = 5.625$ for a square lattice spin $S=1$ monolayer such that the easy axis magnetization $\langle S^z \rangle / S$ comes as close as possible to the magnetization obtained previously [2] with the exchange anisotropy chosen to be $D = 5$. The exchange interaction parameter is $J = 100$, and a small magnetic field in x-direction is used, $B^x = 0.01/S$, which stabilizes the calculation. The comparison is shown in Fig.1.

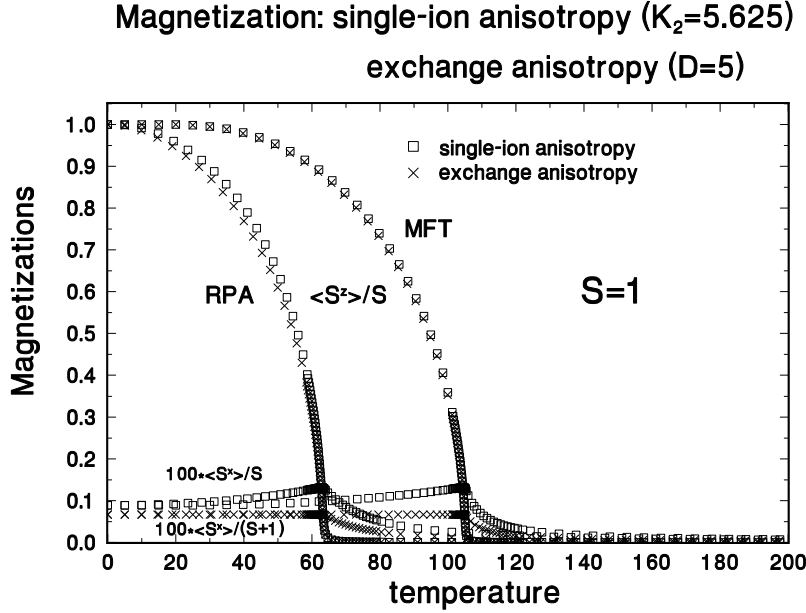


Figure 1: The magnetization $\langle S^z \rangle / S$ of a ferromagnetic spin $S = 1$ Heisenberg monolayer for a square lattice is shown as function of the temperature. Comparison is made between Green's function (RPA) calculations using the exchange anisotropy ($D = 5$, crosses) and the single-ion anisotropy ($K_2 = 5.625$, open squares) with Anderson-Callen decoupling. The corresponding results of mean field (MFT) calculations are also displayed. Also shown are the quantities $100 * \langle S^x \rangle / (S + 1)$ for the exchange anisotropy and $100 * \langle S^x \rangle / S$ for the single-ion anisotropy; the factor 100 is introduced to make the curves visible.

It is surprising that the results for the easy axis magnetization $\langle S^z \rangle$ are very similar over the whole temperature range although the physical origin for the anisotropies is very different. An analogous result was observed for the out-of plane situation discussed in Ref. [3]. The agreement is not so good for the hard axis magnetization, which is a constant for the exchange anisotropy for temperatures below the Curie temperature, whereas it rises slightly up to the Curie temperature when using the

single-ion anisotropy. In Ref.[2] it was shown analytically that the hard axis magnetization is universal for a scaling $\langle S^x \rangle / (S + 1)$ when using the exchange anisotropy. For the single-ion anisotropy a scaling $\langle S^x \rangle / S$ is found to be more appropriate. Comparison is made also with the corresponding mean field (MFT) calculations, obtained by putting $\gamma_{\mathbf{k}} = 0$ in eqn (12), showing the well known shift to larger Curie temperatures (by a factor of about two for the monolayer) due to the missing magnon correlations.

In Figs. 2 and 3 we show the easy and hard axes magnetizations for a monolayer with different spin values S . Whereas one observes in Fig.2 a nearly perfect scaling for the RPA calculations with the exchange anisotropy ($S = 1/2, 1, 3/2, 2, 3, 4, 6, 13/2$, from Ref.[2]) and a universal Curie temperature $T_C(S)$ for RPA and MFT, this is not the case for the corresponding results with the single-ion anisotropy shown for $S = 1, 3/2, 4, 5$ in Fig.3, although the violation of scaling is not dramatical.

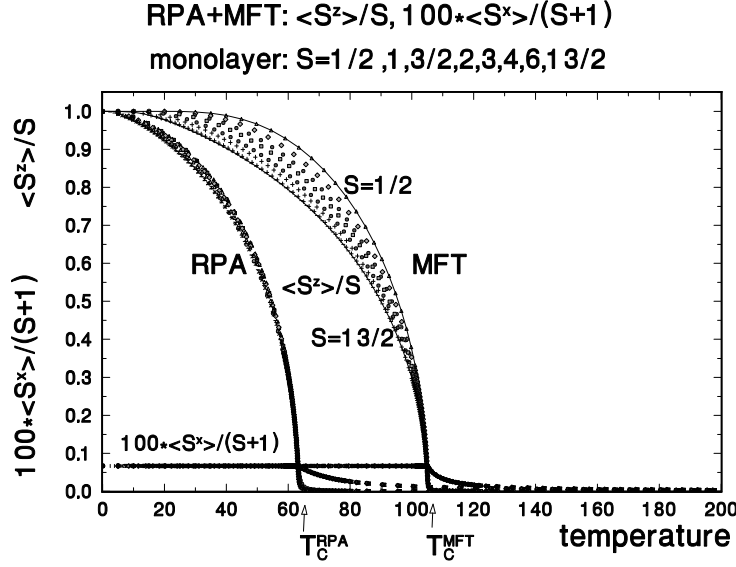


Figure 2: The magnetizations $\langle S^z \rangle / S$ of spin $S = 1/2, 1, 3/2, 2, 3, 4, 6, 13/2$ Heisenberg monolayers for a square lattice are shown as functions of the temperature, from Ref. [2]. Comparison is made between Green's function (RPA) calculations and results of mean field theory (MFT), using the exchange anisotropy strength, $D = 5$. Also shown is the hard axis magnetization, which scales to a universal curve when using $100 * \langle S^x \rangle / (S + 1)$, where the factor 100 is introduced to make the curves visible.

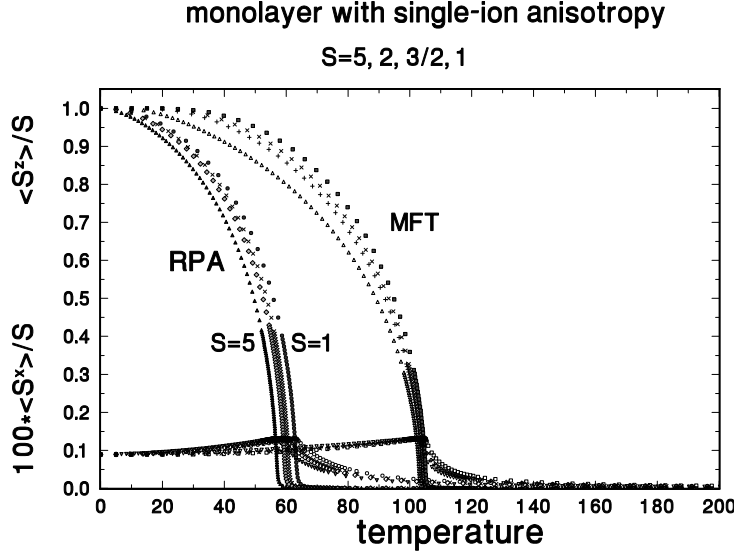


Figure 3: The magnetizations $\langle S^z \rangle / S$ of ferromagnetic spin $S = 1, 2, 3/2, 5$ Heisenberg monolayers for a square lattice are shown as functions of the temperature. Comparison is made between Green's function (RPA) calculations using the single-ion anisotropy strength of $K_2 = 5.625$, and the corresponding results of mean field theory (MFT). Also shown are the quantities $100 * \langle S^x \rangle / S$; the factor 100 is introduced to make the curves visible. There is only an approximate scaling behaviour.

Turning to the inverse easy and hard axes susceptibilities χ_{zz}^{-1} and χ_{xx}^{-1} we find very similar results for the exchange anisotropy and the single-ion anisotropy. In particular in the paramagnetic region ($T > T_{\text{Curie}}$) one has a curved behaviour as function of the temperature for the susceptibilities in RPA due to the presence of spin waves, whereas the corresponding MFT calculations show a Curie-Weiss (linear in the temperature) behaviour due to missing magnon excitations. One observes a slightly less universal behaviour for the results for the single-ion anisotropy, in Fig. 4 and 5, when comparing with the results of the exchange anisotropy, see Figs. 2 and 3 of Ref. [2]. This is connected with the fact that using the exchange anisotropy one finds universal values for the Curie temperatures $T_C^{\text{RPA}}(S)$ and $T_C^{\text{MFT}}(S)$, which is not strictly the case when using the single-ion anisotropy, see Fig. 3. We were also able to show analytically in Ref. [2] that $\chi_{xx}^{-1} * S(S+1)$ is universal for $T < T_C$ when using the exchange anisotropy; this is not the case for the single-ion anisotropy. The only difference concerns the curves for the not perfectly scaled RPA results for χ_{zz}^{-1} : with the exchange anisotropy the curve with the lowest spin value is left from the curves with the higher spin values, whereas the inverse is true for the exchange

anisotropy, but this is not a very pronounced effect, and does not lead to a significant difference between the results for the various anisotropies.

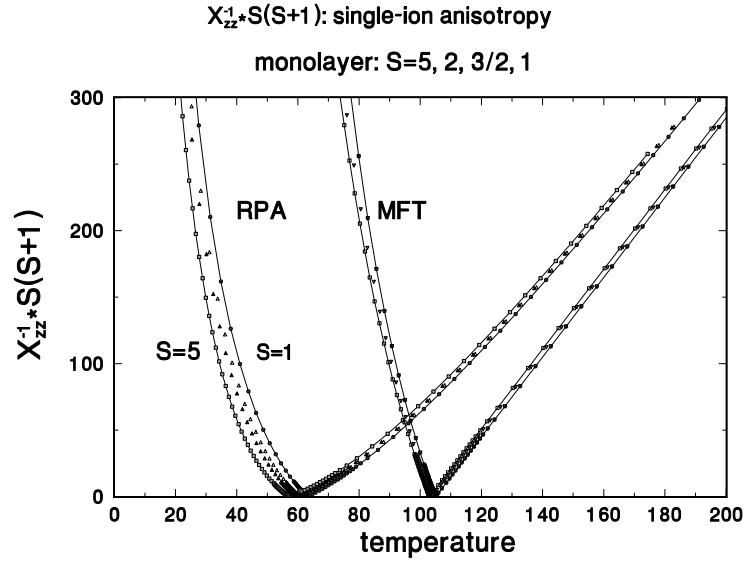


Figure 4: ‘Universal’ inverse easy axis susceptibilities $\chi_{zz}^{-1} * S(S + 1)$ of an in-plane anisotropic (due to the single-ion anisotropy) ferromagnetic square lattice Heisenberg monolayer as functions of the temperature for spins $S = 5, 2, 3/2, 1$. Comparison is made between Green’s function (RPA) and mean field (MFT) calculations.

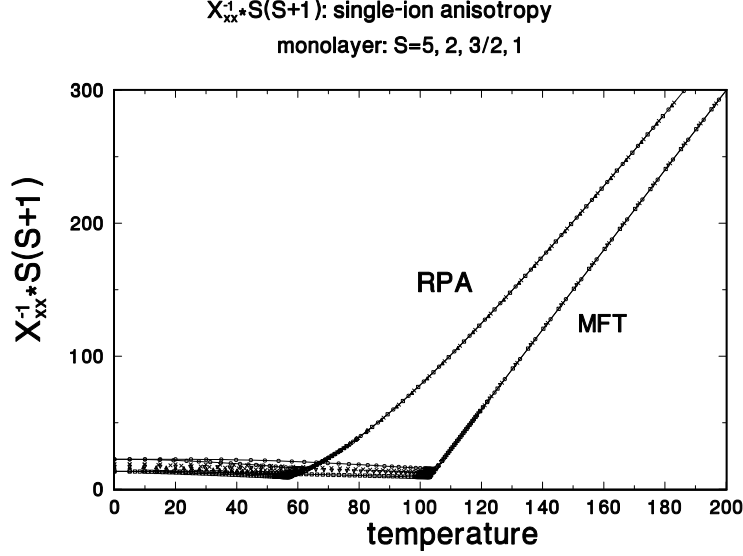


Figure 5: ‘Universal’ inverse hard axis susceptibilities $\chi_{xx}^{-1} * S(S+1)$ of an in-plane anisotropic (due to the single-ion anisotropy) ferromagnetic square lattice Heisenberg monolayer as functions of the temperature for spins $S = 5, 2, 3/2, 1$. Comparison is made between Green’s function (RPA) and mean field (MFT) calculations.

3.2 Multilayers at fixed spin $S = 1$

In discussing multilayers with the exchange anisotropy we have considered only the case of $S = 1/2$ in Ref. [2]. In order to compare with results from the single-ion anisotropy we have to use a larger spin value because $S = 1/2$ is not active in this case. We restrict ourselves to spin $S=1$ in the following. We have performed also calculations with $S > 1$ which scale with respect to the spin in the same way as in the monolayer case.

In Fig. 6 we compare the Curie temperatures for $S = 1$ multilayers for exchange and single-ion anisotropies in RPA and MFT, using for each layer the same parameters as for the monolayer. Remember that the parameters were fixed such that the Curie temperatures for both anisotropies coincide for the monolayer. The Curie temperatures for the multilayers $N = 2, \dots, 19$ (for $N=19$ one is already close to the bulk limit) are only slightly lower for the single-ion anisotropy than those for the exchange anisotropy.

In Figs. 7 and 8 we compare easy and hard axes inverse susceptibilities calculated with single-ion and exchange anisotropy also for the multilayer case. In order to avoid cluttering the figures we restrict ourselves to a multilayer with $N=9$ layers

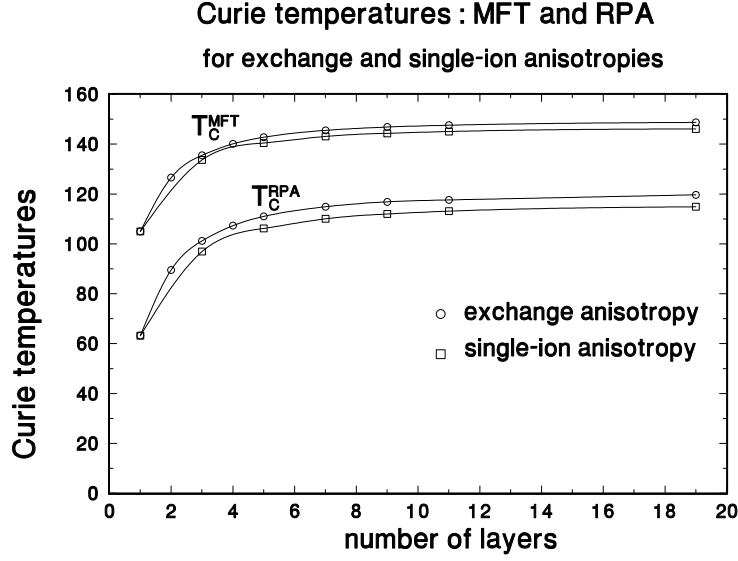


Figure 6: Curie temperatures of ferromagnetic spin $S=1$ multilayers are shown as function of the film thickness for RPA and MFT using the exchange (open circles) and the single-ion (black square) anisotropies.

and spin $S = 1$. For $N > 9$ the corresponding curves would shift only slightly in accordance with the saturation of T_C , see Fig. 6, with increasing film thickness. We display only the RPA results for the multilayer ($N=9$) and compare with the RPA monolayer ($N=1$) result. Again there is no significant difference in the results for both anisotropies. We do not plot the corresponding mean field results which are shifted to higher temperatures and show in the paramagnetic region only a linear in T Curie-Weiss behaviour, whereas the RPA results have curved shapes due to the influence of magnon correlations, which are completely absent in MFT.

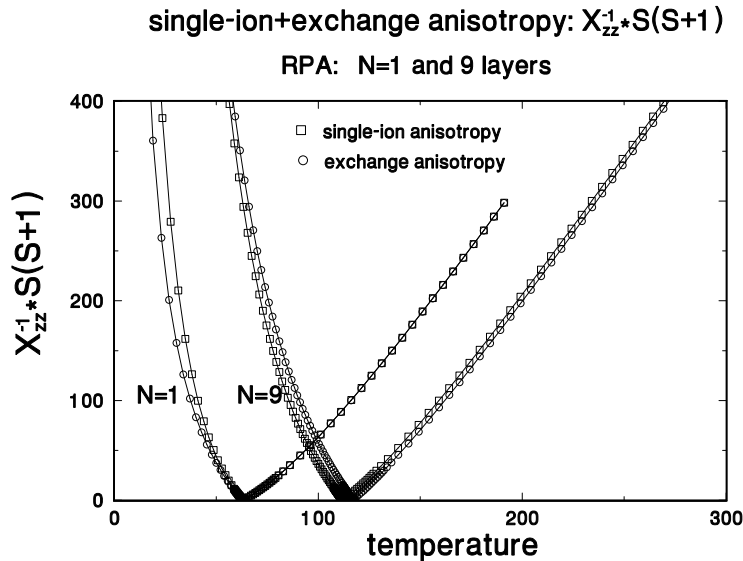


Figure 7: The inverse easy axis susceptibilities χ_{zz}^{-1} of ferromagnetic films in RPA for spin $S = 1$ for a monolayer ($N=1$) and a multilayer ($N=19$) as functions of the temperature for single-ion and exchange anisotropies.

4. Summary and conclusions

We have applied in this paper a many-body Green's function formalism to calculate in-plane anisotropic static susceptibilities of ferromagnetic Heisenberg films using the single-ion anisotropy, and compared with previous calculations [2] in which an exchange anisotropy was used. Although both kinds of anisotropies are of very different physical origin, it is possible, by fitting the strengths of the anisotropies properly, to obtain nearly identical values for the easy axis magnetizations over the complete temperature range for an $S = 1$ monolayer. Using the parameters obtained in this way also for monolayers with higher spin values and for multilayers, we looked for differences in the results of calculations with both kinds of anisotropies.

By using scaled variables we find a fairly universal (independent of the spin quantum number S) of easy and hard axes magnetizations and inverse susceptibilities. Universality is better established for the exchange anisotropy; e.g. we find a universal Curie temperature $T_C(S)$ for RPA and MFT. The scaling is not as perfect for the single-ion anisotropy, but there are *no* dramatic deviations, which might lead to a distinction of the influence of both anisotropies. The general statement made in Ref. [2] that it is sufficient to do a calculation for a particular S and then to apply scaling to obtain the results for other spin values, remains valid to a large extent also for the use of the single-ion anisotropy. It remains also true that the measurement of the hard axis susceptibility gives in principle the possibility to obtain together

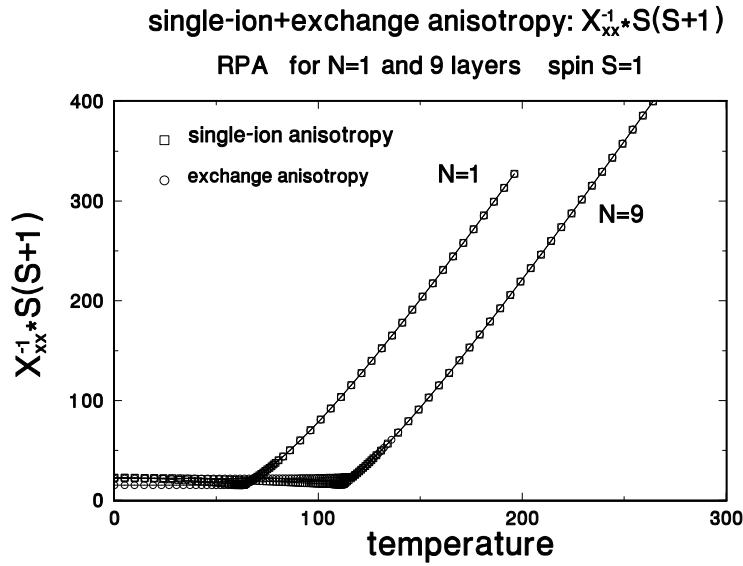


Figure 8: The inverse hard axis susceptibilities χ_{xx}^{-1} of ferromagnetic films in RPA for spin $S = 1$ for a monolayer ($N=1$) and a multilayer ($N=19$) as functions of the temperature for single-ion and exchange anisotropies.

with a measurement of the Curie temperature information on the parameters of the model, the exchange interaction and the anisotropy strengths. One should, however, keep in mind that the quantitative results of the present calculations are due to the use of a square lattice. They could change significantly by using different lattice types and also by layer-dependent exchange interactions and anisotropies. Such calculations are possible, because the numerical program is written in such a way that layer-dependent coupling constants can be used.

As a general result we state that our investigations up to now have *not* lead to any significant differences for the calculated observables (easy and hard axes magnetizations and susceptibilities) when using on one hand the single-ion anisotropy and on the other hand the exchange anisotropy. Therefore it is not possible on the basis of our results to propose an experiment that could decide which kind of anisotropy is acting in an actual ferromagnetic film.

References

- [1] P.J. Jensen, S. Knappmann, W. Wulfhekel, H.P. Oepen, Phys. Rev. B **67**, 184417 (2003).
- [2] P. Fröbrich, P.J. Kuntz, cond-mat/0306243, submitted to Phys. Rev. B
- [3] P. Fröbrich, P.J. Kuntz, Eur. Phys. J. B **32**, 445 (2003).
- [4] P. Fröbrich, P.J. Kuntz, M. Saber, Ann. Phys. (Leipzig) **11**, 387 (2002).
- [5] P. Fröbrich, P.J. Jensen, P.J. Kuntz, A. Ecker, Eur. Phys. J. B **18**, 579 (2000).
- [6] F.B. Anderson, H.B. Callen, Phys. Rev. **136**, A1068 (1964).
- [7] P. Henelius, P. Fröbrich, P.J. Kuntz, C. Timm, P.J. Jensen, Phys. Rev. B **66**, 094407 (2002).
- [8] P. Fröbrich, P.J. Jensen, P.J. Kuntz, Eur. Phys. J. B **13**, 477 (2000).
- [9] M.E. Lines, Phys. Rev. **156**, 534 (1967).
- [10] H.B. Callen, Phys. Rev. **130**, 890 (1963).
- [11] W. Gasser, E. Heiner, and K. Elk, in 'Greensche Funktionen in der Festkörper- und Vielteilchenphysik', Wiley-VHC, Berlin, 2001, Chapter 3.3.
- [12] P. Fröbrich, P.J. Kuntz, Phys. Rev. B **68**, 014410 (2003).